Analytical Approaches to a Disc-Loaded Cylindrical Waveguide for Potential Application in Wide-band Gyro-TWTs

Vishal Kesari, P. K. Jain, and B. N. Basu

***Abstract*—An all-metal disc-loaded cylindrical waveguide excited in TE modes was cold-analyzed in the fast-wave regime for dispersion characteristics, keeping in view of its potential application as an interaction structure for wide-band gyro-traveling-wave tubes (TWTs). The analysis was carried out considering the standing and propagating waves in the disc-occupied and disc-free regions, respectively, using three approaches which differ from one another with respect to how they process the boundary conditions at the interface between these two regions. One such approach is capable of including higher order harmonics in both the structure regions. An adequate number of harmonics with reference to the two regions was taken in the calculation to ensure the convergence of results. The results have been validated against available published results based on different other approaches. The passband and shape of the dispersion characteristics both depend on the disc-hole radius and periodicity, being more sensitive to the latter. The adjustment of disc parameters led to the widening of the straight-line portion of ω-β dispersion characteristics, for wide-band coalescence between the beam-mode and waveguide-mode dispersion characteristics of a gyro-TWT as required for wide-band device performance.**

***Index Terms*—Disc-loaded waveguide, gyrotron, periodic electromagnetic structure, wide-band gyro-traveling-wave tube (TWT).**

I. Introduction

MODIFYING the characteristics of a smooth-wall cylindrical waveguide by corrugation has been a well-known practice in microwave engineering [1]–[11]. For instance, the RF phase velocity of a cylindrical waveguide changes due to the loading of the waveguide by axially periodic annular discs projecting radially inward from the waveguide-wall depending upon the mode and depth of corrugation. Typically, for example, the phase velocity of the TM_{01} mode of a disc-loaded cylindrical waveguide decreases if a corrugation depth smaller than a quarter wavelength is introduced, but increases if a corrugation depth between a quarter and half a wavelength is present. Such a structure is used as a slow-wave structure in the linear electron accelerator [1].

Interest in the study of all-metal structures like a disc-loaded cylindrical waveguide that avoids the presence of a dielectric in the structure and the associated problem of dielectric charging and heat generation due to dielectric loss [12]–[14] has been revived after the advent of gyro-traveling-wave tubes (TWTs), which are still in the experimental stage of development and have a potential for wide-band performance and a scope in high information density communication as well as long range and high-resolution radar. Adjusting the disc parameters can control the dispersion characteristics of a disc-loaded cylindrical waveguide in the fast-wave regime. Hence, such a structure has been considered as a potentially wide-band structure for wide-band gyro-TWTs.

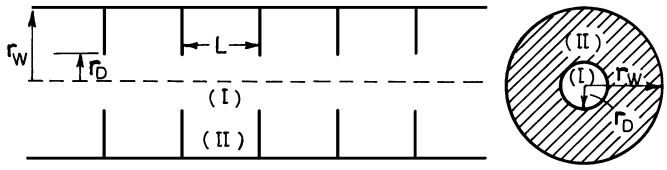

Fig. 1. Schematic of a cylindrical waveguide loaded with annular discs.

The basic method of analysing a disc-loaded waveguide, which is essentially a periodic structure (Fig. 1), that considers the effects of space harmonics due to the axial periodicity of the structure is outlined in the literature [1]–[5]. In this method, the structure is considered as a series of coupled unit cells supporting standing waves in the disc-occupied region and propagating waves in the disc-free region. A surface impedance model is in vogue for the analysis of a disc-loaded cylindrical waveguide, for closely spaced discs, in which the surface impedance is matched at the interface between the corrugation and corrugation-free regions, the interface being treated as a homogeneous reactive surface [3], [9]–[11]. Amari *et al.* [15] analyzed a disc-loaded cylindrical waveguide by coupled-integral-equation technique [16] in which the propagation constants of Floquet's modes are determined from the classical eigenvalues of a characteristic matrix instead of a nonlinear determinantal equation. The analysis of a corrugated rectangular waveguide based on the scattering matrix formalism due to Wagner *et al.* [17] can take into account the precise shape of the corrugation profile.

In the pioneer work of Choe and Uhm [5] the problem has been studied by considering infinitesimally thin annular discs and taking only the lowest order, standing-wave mode in the disc-occupied region and only the fundamental, traveling-wave mode in the disc-free region. Hence, they studied the dependence of the shape of dispersion characteristics of the waveguide on the disc-hole radius and periodicity—a study that is useful in

Manuscript received February 24, 2004; revised July 7, 2003.

The authors are with the Centre of Research in Microwave Tubes, Department of Electronics Engineering, Institute of Technology, Banaras Hindu University, Varanasi 221005, India (e-mail: vishal_kesari@rediffmail.com; bnbasu@bhu.ac.in).

Digital Object Identifier 10.1109/TPS.2004.835518

broadbanding a gyro-TWT by increasing the coalescence bandwidth between the beam-mode and waveguide-mode dispersion characteristics of the device. The objective of this paper is to consider in the analysis higher order harmonics in both the disc-free and disc-occupied regions and, thus, to present the dispersion characteristics of the structure modified over those ignoring such higher order harmonics.

We have made three approaches labeled as approach 1, 2, and 3 (Section II) to the problem that differ or compete with one another with respect to: 1) how they process the boundary conditions at the interface between the disc-occupied and disc-free regions; 2) capability of including higher order harmonics in these two regions; and 3) computational time. In approach 1, one can take into account higher order harmonics both in the disc-free and disc-occupied regions. Approaches 2 and 3 are the two alternative approaches that can take into account higher order harmonics in the disc-free region but not in the disc-occupied region of the interaction structure. Thus, all three approaches enjoy more rigor than the one in which higher order harmonics have not been included in any of these structure regions, such as in Choe and Uhm [5].

The dispersion relations of the disc-loaded cylindrical waveguide obtained by approaches 1, 2, and 3 have been derived (Section II) and the dispersion characteristics compared with one another as well as with those previously obtained by other methods due to Choe and Uhm [5], Amari *et al.* [15], and Clarricoats and Olver [3] (Section III). Out of these, approach 1, which enjoys the most rigor with respect to taking into account higher order harmonics, though at the cost of the computational time, has been taken up further to study the effects of the disc-hole radius and periodicity on the dispersion characteristics of the structure (Section III).

II. Analysis

The cylindrical waveguide loaded with annular metal discs may be considered as a series of coupled unit cells (Fig. 1). The analysis is carried out assuming that standing waves will be formed in the disc-occupied region of each unit cell due to reflection of electromagnetic waves from the metal discs [1], [2]. For the analysis, the disc-loaded cylindrical waveguide is divided into two free-space regions—the disc-free region, labeled as region I, and the disc-occupied region, labeled as region II. In the structure (Fig. 1), region I occupies $0 \le r < r_D$ and $0 < z < \infty$ while region II occupies $r_D \le r < r_W$ and $0 < z < L$, where r_D is the disc-hole radius and r_W is the waveguide-wall radius. L is the axial periodicity of discs supposedly infinitesimally thin as considered in [5].

The field expressions are developed for regions I and II, which are subsequently used along with the boundary conditions at the interface between the two regions to obtain the dispersion relation of the structure. The dispersion relation is used to study the control of the dispersion characteristics of the structure by the disc parameters.

A. Field Expressions

The present analysis is restricted to only TE modes ($E_z = 0$). This is because in a gyro-TWT, for which the waveguide is meant, operates at or near the grazing intersection between the beam-mode and waveguide-mode dispersion characteristics where the TM-mode ($H_z = 0$) growth rate vanishes [18]. Therefore, the relevant field expressions for TE modes in the two regions of the structure in the cylindrical system of coordinates (r, θ, z) may be written for nonazimuthally varying mode $(\partial/\partial\theta = 0)$ and under fast-wave consideration [5], as follows. For region I

$$H_z^I = \sum_{n=-\infty}^{\infty} A_n^I J_0\left\{\gamma_n^I r\right\} \exp j\left(\omega t - \beta_n^I z\right) \tag{1}$$

$$E_\theta^I = \sum_{n=-\infty}^{\infty} \frac{j\omega\mu_0}{\gamma_n^I} A_n^I J_0'\left\{\gamma_n^I r\right\} \exp j\left(\omega t - \beta_n^I z\right). \tag{2}$$

For region II

$$H_z^{II} = \sum_{m=1}^{\infty} A_m^{II} Z_0\left\{\gamma_m^{II} r\right\} \exp(j\omega t) \sin\left(\beta_m^{II} z\right) \tag{3}$$

$$E_\theta^{II} = \sum_{m=1}^{\infty} \frac{j\omega\mu_0}{\gamma_m^{II}} A_m^{II} Z_0'\left\{\gamma_m^{II} r\right\} \exp(j\omega t) \sin\left(\beta_m^{II} z\right) \tag{4}$$

where

$$Z_0\left\{\gamma_m^{II} r\right\} = \frac{\left[Y_0'\left\{\gamma_m^{II} r_W\right\} J_0\left\{\gamma_m^{II} r\right\} - J_0'\left\{\gamma_m^{II} r_W\right\} Y_0\left\{\gamma_m^{II} r\right\}\right]}{Y_0'\left\{\gamma_m^{II} r_W\right\}}$$

$$Z_0'\left\{\gamma_m^{II} r\right\} = \frac{\left[Y_0'\left\{\gamma_m^{II} r_W\right\} J_0'\left\{\gamma_m^{II} r\right\} - J_0'\left\{\gamma_m^{II} r_W\right\} Y_0'\left\{\gamma_m^{II} r\right\}\right]}{Y_0'\left\{\gamma_m^{II} r_W\right\}}.$$

The superscripts I and II refer to regions I and II, respectively. J_0 and Y_0 are the zeroth order Bessel functions of the first and second kinds, respectively, and the prime with these functions indicates their derivative with respect to the argument. Here, referring respectively to regions I and II, A_n and A_m are the field constants, $\gamma_n^I (= [k^2 - (\beta_n^I)^2]^{1/2})$ and $\gamma_m^{II} (= [k^2 - (\beta_m^{II})^2]^{1/2})$ are the radial propagation constants, and β_n^I and β_m^{II} are the axial phase propagation constants, $k (= \omega(\mu_0\varepsilon_0)^{1/2})$ being the free-space propagation constant. n represents the space harmonic number referring to region I, the space harmonics being generated due to the axial periodicity of the structure. m is the modal harmonic number referring to region II, it being assumed that standing waves are supported in region II due to reflection of waves at the discs [1], [2], [5].

A Bessel function of the second kind does not appear in (1) and (2) to prevent fields from blowing up to infinity, in view of the nature of the function: $Y_0\{x\} \to \infty$ and $Y_0'\{x\} \to \infty$, as $x \to 0$. Further, in (3) and (4), the boundary condition $E_\theta^{II} = 0$ at the metallic wall of the boundary $(r = r_W)$ is implied.

Also, since the structure coincides with itself as it is translated through an axial distance equal to the axial periodicity of the structure L, one may relate β_n^I to the axial harmonic number n with the help of Floquet's theorem as [1]

$$\beta_n^I = \beta_0^I + \frac{2\pi n}{L}. \tag{5}$$

Similarly, since region II supports standing waves at $L = m\lambda/2$, λ being the guide wavelength, one may relate the standing wave modal number m to β_m^{II} as [2], [5]

$$\beta_m^{II}\left(=\frac{2\pi}{\lambda}\right)=\frac{m\pi}{L}. \tag{6}$$

B. Dispersion Relation

In order to obtain the dispersion relation of a cylindrical waveguide loaded with annular discs we have used here three different approaches (as mentioned in Section I) which differ with respect to how they process the boundary conditions at the interface between regions I and II, and the capability of including harmonics in these two regions. In principle, approach 1 can take into account the space harmonic numbers $n = 0, \pm1, \pm2, \pm3, \ldots, \pm\infty$, in region I and the standing wave modal numbers, $m = 1, 2, 3, 4, \ldots, \infty$, in region II. In approaches 2 and 3 each, though one can take $n = 0, \pm1, \pm2, \pm3, \ldots, \pm\infty$ in region I, one can consider only the fundamental mode $m = 1$ in region II. These two approaches differ with respect to how they process the boundary conditions, as has been described later in this section.

In approach 1, the field expressions (1)–(4) are substituted into the following boundary conditions stating respectively the continuity of the axial magnetic field intensity and the azimuthal electric field intensity at the interface between the regions I and II

$$\left.\begin{aligned} H_z^I &= H_z^{II} \quad \text{(a)} \\ E_\theta^I &= E_\theta^{II} \quad \text{(b)} \end{aligned}\right\} (r = r_D; 0 < z < L) \tag{7}$$

to obtain

$$\sum_{n=-\infty}^{\infty} A_n^I J_0\left\{\gamma_n^I r_D\right\}\exp\left(-j\beta_n^I z\right) = \sum_{m=1}^{\infty} A_m^{II} Z_0\left\{\gamma_m^{II} r_D\right\}\sin\left(\beta_m^{II} z\right) \tag{8}$$

and

$$\sum_{n=-\infty}^{\infty} \frac{1}{\gamma_n^I} A_n^I J_0'\left\{\gamma_n^I r_D\right\}\exp\left(-j\beta_n^I z\right) = \sum_{m=1}^{\infty} \frac{1}{\gamma_m^{II}} A_m^{II} Z_0'\left\{\gamma_m^{II} r_D\right\}\sin\left(\beta_m^{II} z\right). \tag{9}$$

Multiplying (8) by $\sin(\beta_m^{II} z)$ and integrating it from $z = 0$ to L and using the orthogonal properties of trigonometric functions, an expression for A_m^{II} in the form of a series involving A_n^I $(-\infty < n < \infty)$ may be obtained as follows:

$$A_m^{II} = \sum_{n=-\infty}^{\infty} A_n^I P_{nm} \quad (m = 1, 2, 3, \ldots) \tag{10}$$

where

$$P_{nm} = \frac{2}{L}\frac{J_0\left\{\gamma_n^I r_D\right\}}{Z_0\left\{\gamma_m^{II} r_D\right\}}\frac{\beta_m^{II}\left[1-(-1)^m\exp\left(-j\beta_0^I L\right)\right]}{\left[\left(\beta_m^{II}\right)^2-\left(\beta_n^I\right)^2\right]}. \tag{11}$$

Similarly, multiplying (9) by $\sin(\beta_m^{II} z)$ and proceeding as discussed following (9), one may obtain another expression for A_m^{II} in the form of another series involving A_n^I as follows:

$$A_m^{II} = \sum_{n=-\infty}^{\infty} A_n^I Q_{nm} \quad (m = 1, 2, 3, \ldots) \tag{12}$$

where

$$Q_{nm} = \frac{2}{L}\frac{\gamma_m^{II}}{\gamma_n^I}\frac{J_0'\left\{\gamma_n^I r_D\right\}}{Z_0'\left\{\gamma_m^{II} r_D\right\}}\frac{\beta_m^{II}\left[1-(-1)^m\exp\left(-j\beta_0^I L\right)\right]}{\left[\left(\beta_m^{II}\right)^2-\left(\beta_n^I\right)^2\right]}.$$

Equating the right hand sides of (10) and (12), one obtains

$$\sum_{n=-\infty}^{\infty} A_n^I \alpha_{n,m} = 0 \tag{13}$$

where

$$\alpha_{n,m} = \frac{1}{\left(\beta_m^{II}\right)^2-\left(\beta_n^I\right)^2}\left[\frac{1}{\gamma_n^I}\frac{J_0'\left\{\gamma_n^I r_D\right\}}{Z_0'\left\{\gamma_m^{II} r_D\right\}}-\frac{1}{\gamma_m^{II}}\frac{J_0\left\{\gamma_n^I r_D\right\}}{Z_0\left\{\gamma_m^{II} r_D\right\}}\right]. \tag{14}$$

With the help of (13), one can form a series equation each for each value of m considered. Thus m such series equations in field constants can be formed. Taking the same number of values, say, s of standing wave modal number m as that of space harmonic number n (for instance, $n = 0$, ±1,±2, ±3, and $m =$ 1, 2, 3, 4, 5, 6, 7, corresponding to $s = 7$), one may then find the dispersion relation as the condition for the existence of a nontrivial solution in the form of a determinant put equal to zero as follows:

$$\det\left|\alpha_{n,m}\right| = 0 \quad (-\infty < n < \infty, 1 \le m < \infty; \text{approach 1}) \tag{15}$$

where α_{nm} represents the element at the intersection between the mth row and the $(n+(s+1)/2)$th column of the determinant.

In approach 2, starting from (8), as discussed following (9), one has to obtain the same expression as (10) for A_m^{II} in the form of a series involving A_n^I $(-\infty < n < \infty)$. However, in addition, now one has to obtain an expression for A_n^I in the form of a series involving A_m^{II} $(1 \le m < \infty)$. For this, let us first multiply (9), in which β_n^I is interpreted as (5), by $\exp(j\beta_0^I z)$, to obtain

$$\sum_{n=-\infty}^{\infty} \frac{1}{\gamma_n^I} A_n^I J_0'\left\{\gamma_n^I r_D\right\}\exp\left(\frac{-j2n\pi z}{L}\right) = \sum_{m=1}^{\infty} \frac{1}{\gamma_m^{II}} A_m^{II} Z_0'\left\{\gamma_m^{II} r_D\right\}\sin\left(\beta_m^{II} z\right)\exp\left(j\beta_0^I z\right)$$

which is then multiplied by $\exp(j2n\pi z/L)$ and integrated from $z = 0$ to L, while using the orthogonal properties of trigonometric function, to obtain

$$A_n^I = \sum_{m=1}^{\infty} A_m^{II} R_{nm}, \quad (n = 0, \pm1, \pm2, \ldots) \tag{16}$$

where

$$R_{nm} = \frac{1}{L}\frac{\gamma_n^I}{\gamma_m^{II}}\frac{Z_0'\left\{\gamma_m^{II} r_D\right\}}{J_0'\left\{\gamma_n^I r_D\right\}}\frac{\beta_m^{II}\left[(-1)^m\exp\left(j\beta_0^I L\right)-1\right]}{\left[\left(\beta_n^I\right)^2-\left(\beta_m^{II}\right)^2\right]}. \tag{17}$$

Substitution of (16) into (10) yields

$$A_m^{II} = \sum_{n=-\infty}^{+\infty} \sum_{m=1}^{+\infty} A_m^{II} R_{nm} P_{nm}. \tag{18}$$

Putting in (18) all A_m^{II}s equal to zero except A_1^{II} $(m = 1)$, which amounts to taking only the lowest standing-wave mode in region II, as has been done in [2] with reference to a general analysis of a two-dimensional planar periodic structure, one obtains

$$1 - \sum_{n=-\infty}^{+\infty} R_{n1} P_{n1} = 0$$

which may be read with the help of (11) and (17) to obtain the dispersion relation of the structure as follows:

$$\sum_{n=-\infty}^{+\infty} \gamma_n^I \frac{J_0\{\gamma_n^I r_D\}}{J_0'\{\gamma_n^I r_D\}} \frac{1}{\left[\left(\frac{\pi}{L}\right)^2 - (\beta_n^I)^2\right]^2} = \frac{\gamma_1^{II} \exp\left(j\beta_0^I L\right)}{\left[1 + \exp\left(j\beta_0^I L\right)\right]^2} \frac{L^4}{2\pi^2} \frac{Z_0\{\gamma_1^{II} r_D\}}{Z_0'\{\gamma_1^{II} r_D\}} \quad (-\infty < n < \infty, m = 1; \text{approach 2}). \tag{19}$$

In approach 3, the standing wave corresponding only to $m = 1$ is considered as discussed with reference to approach 2 following (18). Here, the expression for H_z^I from (1) and that for H_z^{II} from (3), the latter interpreted for $m = 1$, are substituted into (7a) at the axial position $z = L/2$, the midpoint at the interface between regions I and II [1], to obtain an expression for A_1^{II} in the form of a series involving A_n^I $(-\infty < n < \infty)$ as follows:

$$A_1^{II} = \frac{1}{Z_0\{\gamma_1^{II} r_D\}} \sum_{n=-\infty}^{\infty} A_n^I J_0\{\gamma_n^I r_D\} \exp\left(-j\beta_0^I \frac{L}{2}\right). \tag{20}$$

Further, multiplying both sides of (9), the latter interpreted for $m = 1$, by $\exp(j\beta_n^I z)$ and integrating it from $z = 0$ to L, one obtains A_n^I in terms of A_1^{II} as

$$A_n^I = \frac{\pi}{L^2} \frac{\gamma_n^I}{\gamma_1^{II}} \frac{Z_0'\{\gamma_1^{II} r_D\}}{J_0'\{\gamma_n^I r_D\}} \frac{\left(\exp\left(j\beta_0^I L\right) + 1\right)}{\left[\left(\frac{\pi}{L}\right)^2 - (\beta_n^I)^2\right]} A_1^{II}. \tag{21}$$

Substituting A_n^I from (21) into (20), one obtains the dispersion relation of the structure as

$$\sum_{n=-\infty}^{\infty} \gamma_n^I \frac{J_0\{\gamma_n^I r_D\}}{J_0'\{\gamma_n^I r_D\}} \frac{\cos\left(\beta_0^I \frac{L}{2}\right)}{\left[\left(\frac{\pi}{L}\right)^2 - (\beta_n^I)^2\right]} = \gamma_1^{II} \frac{L^2}{2\pi} \frac{Z_0\{\gamma_1^{II} r_D\}}{Z_0'\{\gamma_1^{II} r_D\}}. \quad (-\infty < n < \infty, m = 1; \text{approach 3}). \tag{22}$$

III. Results and Discussion

As a special case of the disc-hole radius being equal to the waveguide-wall radius $(r_D = r_W)$, the function Z_0' appearing in each of the dispersion relations (15), (19), and (22), obtained by approaches 1, 2, and 3, respectively, becomes zero which in turn will lead each of these dispersion relations to the one and the same relation $J_0'\{\gamma_n^I r_W\} = 0$, which may be identified with the characteristic equation of a smooth-wall cylindrical waveguide excited in nonazimuthally varying TE modes.

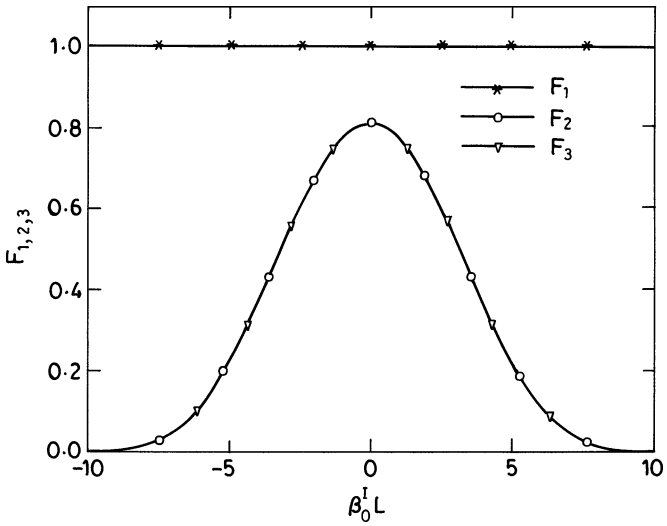

Fig. 2. Variation of the factors $F_{1,2,3}$, which appear in the special case ($n = 0$; $m = 1$) of the dispersion relation, with $\beta_0^I L$.

Further, it is of interest to compare the dispersion relation obtained by the present analysis using the three approaches 1, 2, and 3 with that obtained by Choe and Uhm [5]. As a special case ($n = 0$, $m = 1$), the dispersion relations (15), (19), and (22) may be expressed as

$$\frac{\gamma_1^{II} Z_0\{\gamma_1^{II} r_D\}}{Z_0'\{\gamma_1^{II} r_D\}} = \frac{\gamma_0^I J_0\{\gamma_0^I r_D\}}{J_0'\{\gamma_0^I r_D\}} F_{1,2,3} \quad (n = 0 \text{ and } m = 1) \tag{23}$$

where the factors $F_{1,2,3}$ refer to approaches 1, 2, and 3, respectively, and are given by

$$\left.\begin{aligned} F_1 &= 1 && \text{(a)} \\ F_2 &= 2\pi^2 \left[1 + \exp\left(j\beta_0^I L\right)\right]^2 \\ &\quad \times \exp\left(-j\beta_0^I L\right) \left[\pi^2 - \left(\beta_0^I L\right)^2\right]^{-2} && \text{(b)} \\ F_3 &= 2\pi \cos\left(\beta_0^I \tfrac{L}{2}\right) \left[\pi^2 - \left(\beta_0^I L\right)^2\right]^{-1} && \text{(c)} \end{aligned}\right\}. \tag{24}$$

It can be seen from (24) that, while the factor F_1, referring to approach 1 is unity irrespective of the axial periodicity L of discs, the values of the factors F_2 and F_3, referring to approaches 2 and 3, respectively, each depending on L, are very close to one another, and each becoming closer to unity, as $\beta_0^I L \to 0$ (closely spaced discs) (Fig. 2). Thus, it follows from (23), read with the help of (24), that the dispersion relation, as a special case ($n = 0$ and $m = 1$), obtained by approach 1 of the present analysis, exactly passes on to that obtained by Choe and Uhm [5]; however, the dispersion relations obtained by approaches 2 and 3 would each pass on to that obtained by Choe and Uhm [5] though approximately and only for closely spaced discs.

In general, in region I, approaches 1, 2, and 3 [dispersion relations (15), (19), and (22)] include all the space harmonics $n = 0, \pm 1, \pm 2, \pm 3, \ldots, \pm\infty$. However, in region II, only approach 1 [dispersion relation (15)] includes all the standing-wave modal

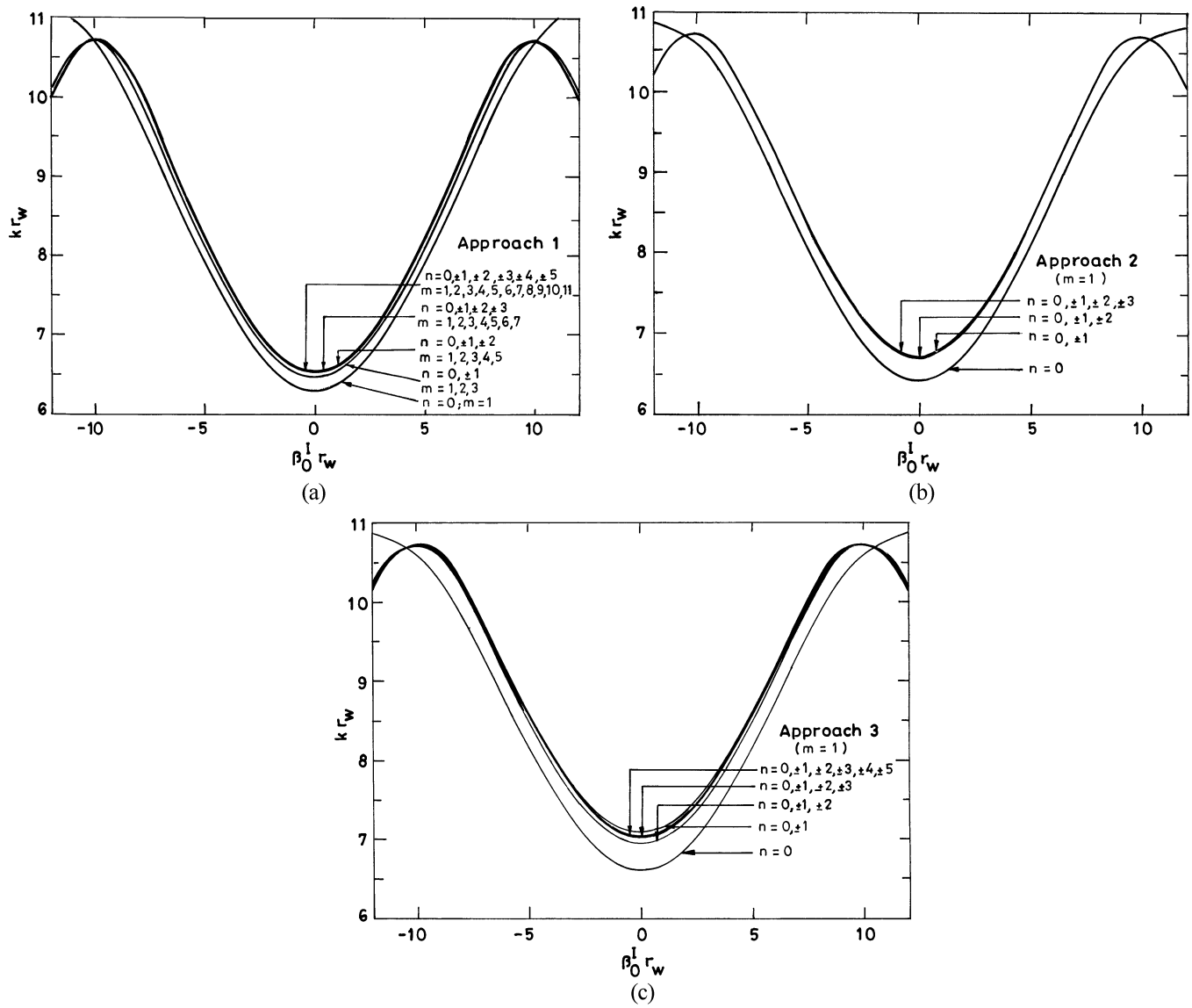

Fig. 3. Effect of including higher order harmonics in (a) approach 1, (b) approach 2, and (c) approach 3, taking typically TE_{01}-mode excitation with disc parameters $r_D/r_W = 0.5$, $L/r_W = \pi/10$.

harmonic numbers $(m = 1, 2, 3, \ldots + \infty)$, whereas approaches 2 and 3 [dispersion relations (19) and (22)] each consider only the lowest order modal number $(m = 1)$. These dispersion relations are solved using numerical methods in the software MATLAB. The dispersion relations (19) and (22) obtained by approaches 2 and 3, respectively, are essentially the series expressions involving infinite number of terms. In MATLAB, the number of terms in the series is increased till the desired convergence solutions are obtained, typically, thus retaining the terms in (19) corresponding to $n = 0, \pm 1, \pm 2, \pm 3, \pm 4$ in approach 2 [Fig. 3(b)] and those in (22) corresponding to $n = 0, \pm 1, \pm 2, \pm 3, \pm 4, \pm 5$ in approach 3 [Fig. 3(c)], for the desired convergence. Similarly, the infinite-order determinant involved in the dispersion relation (15) obtained by approach 1 is truncated typically at 7×7 for the desired converging solutions [Fig. 3(a)].

It is worth comparing the three approaches with one another and also with an approach that considers the lowest order harmonics ($n = 0$ and $m = 1$) [5] [Fig. 4(a)]. Clearly, in general, the values of the cutoff frequency predicted by approaches 1, 2, and 3 are increasingly higher than that predicted for the lowest order harmonics ($n = 0$ and $m = 1$), the percentage difference from the latter being 3.9%, 7.4%, and 11.6%, respectively [Fig. 4(a)]. Further, the dispersion characteristics for typical modes TE_{01} and TE_{02} obtained by approach 1, which enjoys the rigor and flexibility with respect to including higher order values of both n and m in the analysis over the other two approaches (2 and 3), have been validated against those obtained by Amari *et al.* [15] and Clarricoat and Olver [3]. The dispersion characteristics obtained by approach 1 very closely agreed with those of Amari *et al.* [15] both at the cutoff frequency and away from it [Fig. 4(b)]. Furthermore, the dispersion characteristics obtained by approach 1 and those by Amari *et al.* [15] have each closely agreed, away from the cutoff, and fairly agreed, at the cutoff (within 2.4%), with Clarricoat and Olver [3] [Fig. 4(b)]. Hence, the characteristics of a disc-loaded cylindrical waveguide have been further investigated here using approach 1 (Fig. 6). Obviously, however, as compared to approaches 2 and 3, approach 1 would require more computer run-

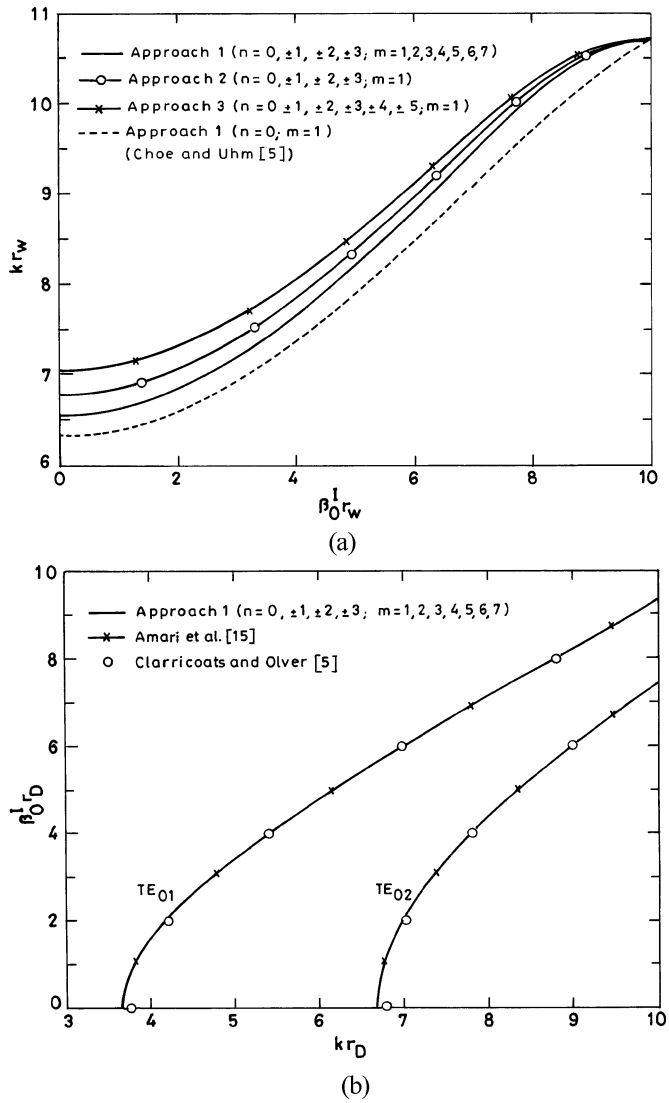

Fig. 4. (a) Comparison of the dispersion characteristics of a cylindrical waveguide loaded with annular discs obtained by approaches 1, 2, and 3 considering higher order harmonics with those obtained ignoring them [5] taking disc parameters $r_D/r_W = 0.5$, $L/r_W = \pi/10$. (b) Validation of approach 1 against Amari *et al.* [15] and Clarricoats and Olver [3] taking disc parameters $r_D/r_W = 0.8$, $L/r_W = 0.2$. [The ordinate and abscissa are suitably adjusted for the sake of comparison with [5] in (a) and with [15] and [3] in (b)].

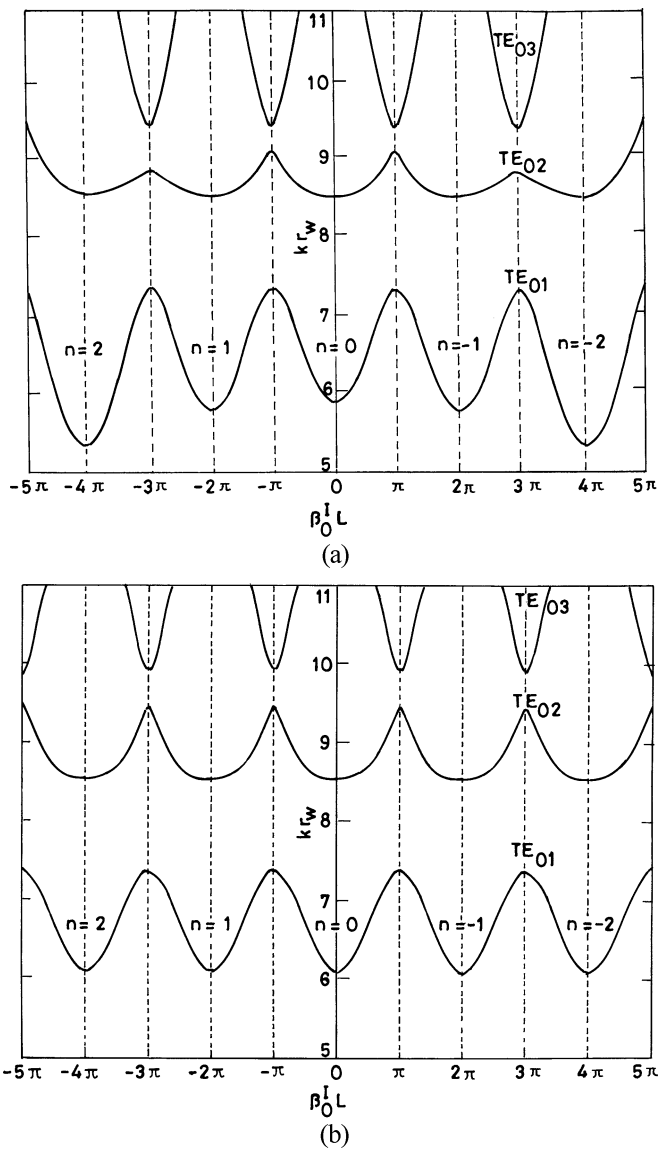

Fig. 5. Pass and stop band characteristics of a cylindrical waveguide loaded with annular discs using approach 1 showing the effect of considering (a) lower order harmonics ($n = 0, \pm1, \pm2$; $m = 1, 2, 3, 4, 5$) and (b) higher order harmonics ($n = 0, \pm1, \pm2, \pm3, \pm4, \pm5$; $m = 1, 2, 3, 4, 5, 6, 7, 8, 9, 10, 11$), taking excitation typically in TE_{01}, TE_{02} and TE_{03} modes with disc parameters $r_D/r_W = 0.5$, $L/r_W = 0.5$.

ning time that would increase with the number of harmonics included in the calculation. For instance, the computation running time would be, typically, ~110 min for $n = 0, \pm1$; $m = 1, 2, 3$ using approach 1, while the same would be ~10 min if either of approaches 2 or 3 $(m = 1)$ were used $(n = 0, \pm1)$. The running time would increase to ~550 min if the number of harmonics were increased to $n = 0, \pm1, \pm2, \pm3, \pm4, \pm5$; $m = 1, 2, 3, 4, 5, 6, 7, 8, 9, 10, 11$ while using approach 1, and the same would be ~15 min, if either of approaches 2 or 3 $(m = 1)$ were used $(n = 0, \pm1, \pm2, \pm3, \pm4, \pm5)$.

At the first instance, the structure has shown the periodic nature of dispersion diagram [1], [2] by exhibiting pass and stop bands at a constant interval of 2π in the value of $\beta_0^I L$ between two consecutive maxima or two consecutive minima (Fig. 5). However, the dispersion diagram fails to become identical at such periodic intervals for lower order harmonics [Fig. 5(a)]. The identicalness of the diagram is exhibited only by including higher order harmonics [Fig. 5(b)].

The dispersion characteristics obtained by the present analysis considering higher order harmonics, typically $n = 0, \pm1, \pm2, \pm3$ and $m = 1, 2, 3, 4, 5, 6, 7$, would be different from and, in fact, more accurate than those obtained by ignoring them, for instance, by taking $n = 0$ and $m = 1$ in our analysis, the latter being identical with those obtainable by Choe and Uhm [5] (Fig. 6).

The cutoff frequency of the waveguide, that is the lower-edge frequency of the passband, increases while the upper-edge frequency of the band remains unchanged, with the decrease of the disc-hole radius relative to waveguide-wall radius r_D/r_W [Fig. 6(a)]. However, the lower- and the upper-edge frequencies

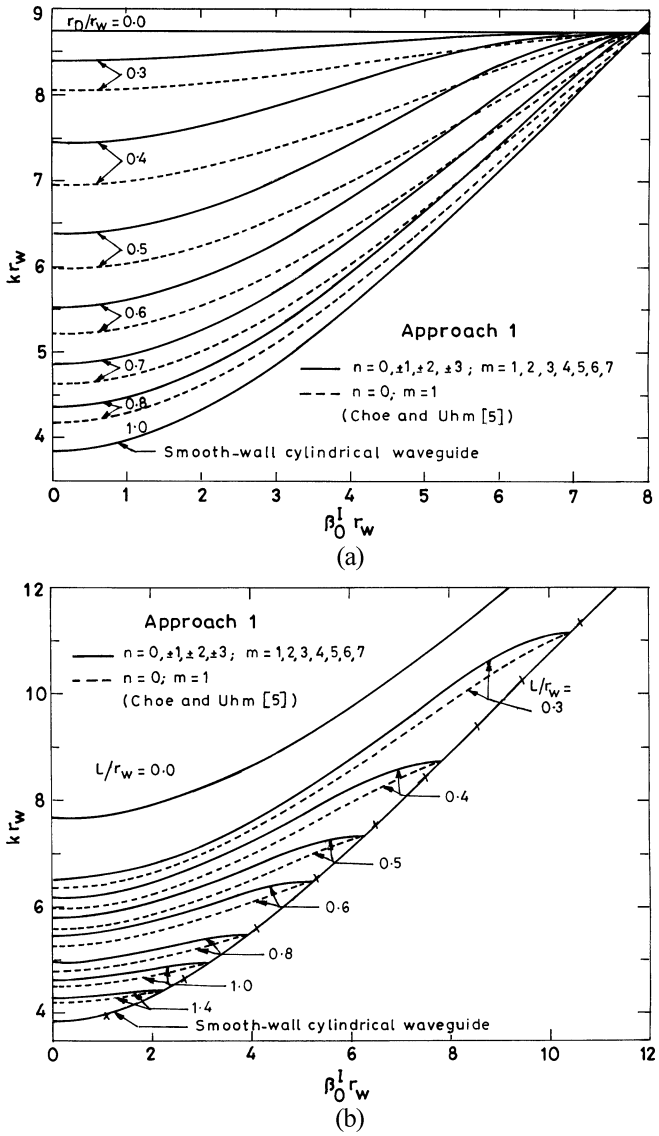

Fig. 6. Dispersion characteristics of a cylindrical waveguide loaded with annular discs typically excited in TE_{01} mode using approach 1 ($n = 0, \pm 1, \pm 2, \pm 3$; $m = 1, 2, 3, 4, 5, 6, 7$) taking as parameters (a) the relative inner edge radius of the annular disc r_D/r_W, typically with $L/r_W = 0.4$, and (b) the relative disc periodicity L/r_W, typically with $r_D/r_W = 0.5$, each compared with those ignoring higher order harmonics taking $n = 0$, $m = 1$ [5], shown by broken curves. The line with crosses in (b) is the locus of the upper-edge frequencies of the passband for different values of L/r_W that coincides with the dispersion characteristics of the corresponding smooth-wall cylindrical waveguide.

each increase with the decrease of the disc periodicity relative to waveguide-wall radius L/r_W [Fig. 6(a)].

It is also of interest to bring out an interesting observation with the lower limiting and the upper limiting cases of disc-hole radius and periodicity. The lower limiting case of disc-hole radius, $r_D/r_W \rightarrow 0$, will correspond to the case of a series of uncoupled cavities between the original positions of discs. In a similar situation for the disc-loaded cylindrical waveguide, though for TM modes, it is given in Watkins [1] that the ω-β dispersion plot would be a straight line parallel to the abscissa (β-axis) at the common lower-edge frequency of the passband for all the values of r_D/r_W. In the present case, too, for TE modes, the same has been observed however now at the common upper-edge frequency of the passband [Fig. 6(a)]. The upper limiting case, $r_D/r_W \rightarrow 1$, will correspond to a smooth-wall cylindrical waveguide [Fig. 6(a)]. The observation may also be extended to the lower limiting case of disc periodicity, $L/r_W \rightarrow 0$, [Fig. 6(b)]. For such a case, $\beta_m^{II}(= m\pi/L) \rightarrow \infty$ which in turn reduces each of the dispersion relations (15) (approach 1), (19) (approach 2) and (22) (approach 3) to $J_0'\{\gamma_n^I r_D\} \rightarrow 0$. The latter may be identified with the TE mode dispersion relation of a smooth-wall cylindrical waveguide of radius r_D (instead of r_W). This is expected of the case of densely populated discs ($L \rightarrow 0$) that may be considered as a cylindrical sheath of infinite and zero conductivities along the azimuthal and axial directions, respectively, which would shield the azimuthal electric field intensity (E_θ^I) at $r = r_D$, and be transparent to the axial electric field intensity which however is absent in the present case in view of the TE mode excitation considered. In other words, for the special case of closely spaced discs, one may model the structure by replacing the discs at their tips ($r = r_D$) by an azimuthally conducting cylindrical sheath [Fig. 6(b)]. The upper limiting case of disc periodicity $L/r_W \rightarrow \infty$ on the other hand, would correspond to the dispersion plot being a straight line (not shown here) parallel to the abscissa (β-axis) at the cutoff frequency of the discs-free or smooth-wall waveguide [Fig. 6(b)]. It is also of interest to note that the upper-edge frequencies of the passband for different axial periodicity values relative to the waveguide wall radius will all lie on the dispersion curve (hyperbola) of the smooth-wall cylindrical waveguide [Fig. 6(b)].

The shape of the dispersion characteristics depends on both the disc-hole radius and periodicity, being more sensitive to the latter (Fig. 6). In order to widen the bandwidth of a gyro-TWT one has to widen the frequency range of the straight-line portion of ω-β dispersion characteristics of the structure and ensure its grazing intersection or coalescence with the beam-mode dispersion line of the device [8], [13], [14], [19]. One has to optimize the disc parameters for widening the coalescence bandwidth preferably near the waveguide cutoff in order to minimize the effect of beam velocity spread in the device. Thus, the disc-hole radius may be decreased [Fig. 6(a)] and the disc periodicity increased [Fig. 6(b)] for widening the device bandwidth. However, such broadbanding of coalescence is accompanied by the reduction of the bandwidth of the passband of the structure itself Fig. 6. It is however felt that in order to fully explore the potential of the present cold (beam-absent) analysis of a disc-loaded cylindrical waveguide and study the effect of the disc parameters on the bandwidth of a gyro-TWT, one has to substitute, as we have done in the past with reference to dielectric loaded and metal vane loaded gyro-TWTs [8], [13], [19], the propagation constant predicted by the present cold analysis into the beam-present dispersion relation of a gyro-TWT and interpret the latter for the gain-frequency characteristics of the device and the dependence thereof on the structure parameters. We have, however, kept such study outside the scope of the present paper.

In this paper, an all-metal structure, namely, a cylindrical waveguide loaded with annular discs has been analyzed in the fast-wave regime in view of the potential application of the structure in widening the bandwidth of a gyro-TWT. The dispersion relation, as special cases, has passed on to that of

a smooth-wall cylindrical waveguide and to that predicted for closely spaced discs by a model that replaces the discs at their tips by an azimuthally conducting cylindrical sheath. Moreover, care has been taken to validate the results of the present analysis against those reported in the literature using other different analytical approaches. Out of the three approaches to the analysis considered here, the one that enjoys most the rigor and flexibility of including higher order of harmonics has been used to study the effect of the disc parameters on the dispersion characteristics of the structure. It is hoped that the study would be use to the developers of wide-band gyro-TWTs.

REFERENCES

[1] D. A. Watkins, *Topics in Electromagnetic Theory*. New York: Wiley, 1958.

[2] R. E. Collin, *Foundation for Microwave Engineering*. New York: McGraw-Hill, 1988.

[3] P. J. B. Clarricoats and A. D. Olver, *Corrugated Horns for Microwave Antennas*. London, U.K.: Peter Peregrinus, 1984.

[4] P. K. Saha and P. J. B. Clarricoats, "Propagation and radiation behavior of corrugated coaxial horn feed," *Proc. Inst. Elect. Eng.*, vol. 118, no. 9, pp. 1177–1186, Sept. 1971.

[5] J. Y. Choe and H. S. Uhm, "Theory of gyrotron amplifiers in disc or helix-loaded waveguides," *Int. J. Electron.*, vol. 53, no. 6, pp. 729–741, Sept. 1982.

[6] G. G. Denisov, V. L. Bratman, A. W. Cross, W. He, A. D. R. Phelps, K. Ronald, S. V. Samsonov, and C. G. Whyte, "Gyrotron travelling wave amplifier with a helical interaction waveguide," *Phys. Rev. Lett.*, vol. 81, no. 25, pp. 5680–5683, Dec. 1998.

[7] C. K. Chong, D. B. McDermott, A. J. Balkcum, and N. C. J. Luhmann Jr., "Nonlinear analysis of high-harmonic slotted gyro-TWT amplifier," *IEEE Trans. Plasma Sci.*, vol. 20, pp. 176–187, June 1992.

[8] M. Agrawal, G. Singh, P. K. Jain, and B. N. Basu, "Analysis of a tapered vane loaded broad-band gyro-TWT," *IEEE Trans. Plasma Sci.*, no. 3, pp. 439–444, June 2001.

[9] H. Li and X. Li, "Analysis and calculation of an electron cyclotron maser having inner and outer slotted structure," *Int. J. Electron.*, vol. 70, no. 1, pp. 213–219, Jan. 1991.

[10] C. T. Iatrou, S. Kern, and A. B. Pavelyev, "Coaxial cavities with corrugated inner conductor for gyrotrons," *IEEE Trans. Microwave Theory Tech.*, vol. 44, pp. 56–64, Jan. 1996.

[11] J. J. Barroso, R. A. Correa, and P. J. de Castro, "Gyrotron coaxial cylindrical resonators with corrugated inner conductor: theory and experiment," *IEEE Trans. Microwave Theory Tech.*, vol. 46, pp. 1221–1230, Sept. 1998.

[12] J. Y. Choe and H. S. Uhm, "Analysis of wide-band gyrotron amplifiers in a dielectric loaded waveguide," *J. Appl. Phys.*, vol. 52, no. 7, pp. 4506–4516, Oct. 1981.

[13] S. J. Rao, P. K. Jain, and B. N. Basu, "Broadbanding of a gyro-TWT by dielectric-loading through dispersion shaping," *IEEE Trans. Electron Devices*, vol. 43, pp. 2290–2299, Dec. 1996.

[14] K. C. Leou, D. B. McDermott, and N. C. Luhmann Jr., "Dielectric loaded wide-band gyro-TWT," *IEEE Trans. Plasma Sci.*, vol. 20, pp. 188–196, June 1992.

[15] S. Amari, R. Vahldieck, and J. Bornemann, "Analysis of propagation in periodically loaded circular waveguides," *Proc. Inst. Elect. Eng. Microwave Antennas Propag.*, vol. 146, no. 1, pp. 50–54, Feb. 1999.

[16] S. Amari, J. Bornemann, and R. Vahldieck, "Accurate analysis of scattering from multiple waveguide discontinuities using the coupled-integral-equations technique," *J. Electromag. Waves Appl.*, vol. 10, no. 12, pp. 1623–1644, Dec. 1996.

[17] D. Wagner, M. Thumm, and W. Kasparek, "Hybrid modes in highly oversized corrugated rectangular waveguides," *Int. J. Infrared Millim. Waves*, vol. 20, no. 4, pp. 567–581, Apr. 1999.

[18] A. W. Fliflet, "Linear and nonlinear theory of the Doppler-shifted cyclotron resonance maser based on TE and TM waveguide modes," *Int. J. Electron.*, vol. 61, no. 6, pp. 1049–1080, Sept. 1986.

[19] S. J. Rao, P. K. Jain, and B. N. Basu, "Two-stage dielectric-loading for broadbanding a gyro-TWT," *IEEE Electron Device Lett.*, vol. 17, pp. 303–305, June 1996.

Vishal Kesari was born in Mughalsarai (Uttar Pradesh), India, in 1978. He received the M.Sc degree in physics from Purvanchal University, Jaunpur, India, in 2001. He is currently working toward the Ph.D. degree in the Department of Electronics Engineering, Institute of Technology, Banaras Hindu University, Varanasi, India.

His research interest includes periodically loaded cylindrical waveguides for slow- and fast-wave vacuum electron devices/tubes.

P. K. Jain received the B.Tech degree in electronics engineering, and the M.Tech. and Ph.D. degrees in microwave engineering, all from Banaras Hindu University (BHU), Varanasi, India, in 1979, 1981, and 1988, respectively.

In 1981, he joined the Centre of Research in Microwave Tubes, Department of Electronics Engineering, Institute of Technology, BHU, as a Lecturer, and is currently working there as a Professor. He was a Principal Investigator of the project "Studies on slow- and fast-wave interaction structures for beam-wave interaction in TWTs," sponsored by the Ministry of Defence. The areas of his current research and publications include CAD/ CAM, modeling and simulation of microwave tubes and their subassemblies, including broadbanding of helix traveling-wave tubes (TWTs), and cyclotron resonance measure devices including gyrotrons and gyro-TWTs and their performance improvement.

Dr. Jain is a Fellow of the Institution of Electronics and Telecommunication Engineers, India.

B. N. Basu received the M.Tech. and Ph.D. degrees from Institute of Radiophysics and Electronics, Calcutta University, Calcutta, India, in 1966 and 1976, respectively.

He is currently Professor and Coordinator at the Centre of Research in Microwave Tubes, Electronics Engineering Department, Banaras Hindu University, Varanasi, India. He was associated with Central Electronics Engineering Research Institute (CEERI), Pilani, Council of Scientific and Industrial Research (CSIR), India, as Distinguished Visiting Scientist of CSIR. He was a partner with University of Lancaster (UoL), U.K. and CEERI under Academic Link and Interchange Scheme (ALIS) between CSIR and British Council and worked at UoL. Also, he worked at Seoul National University, Seoul, Korea as a Visiting Scientist. His areas of current research and publications include helix-traveling-wave tubes (TWTs), gyrotrons, and gyro-TWTs. He has authored or coauthored around 100 research papers in peer-reviewed journals and authored a book entitled "Electromagnetic Theory and Applications in Beam-Wave Electronics" (Singapore: World Scientific, 1996).

Dr. Basu is a Member of the Technical Committee on Vacuum Electron Devices of IEEE Electron Devices Society. He is a Fellow and recipient of S. V. C. Aiya Memorial Award for outstanding contributions in motivating research from the Institution of Electronics and Telecommunication Engineers, India.